NEOPLASIA
www.neoplasia.com
Volume 10 Number 5 May 2008 pp. 462–470 462

Activation of MAP Kinase Signaling Through ERK5 But Not ERK1 Expression Is Associated with Lymph Node Metastases in Oral Squamous Cell Carcinoma (OSCC)[1,2]

Carsten Sticht*,†,3, Kolja Freier*,†,3, Karl Knöpfle*,†, Christa Flechtenmacher‡, Susanne Pungs†, Christof Hofele†, Meinhard Hahn*, Stefan Joos* and Peter Lichter*

*Abteilung Molekulare Genetik (B060), Deutsches Krebsforschungszentrum, Im Neuenheimer Feld 280, D-69120 Heidelberg, Germany; †Klinik für Mund-Kiefer-Gesichtschirurgie, Universitätsklinikum Heidelberg, Im Neuenheimer Feld 400, D-69120 Heidelberg, Germany; ‡Pathologische Institut, Universitätsklinikum Heidelberg, Im Neuenheimer Feld 220, D-69120 Heidelberg, Germany

Abstract

In an attempt to further elucidate the pathomechanisms in oral squamous cell carcinoma (OSCC), gene expression profiling was performed using a whole-transcriptome chip that contains 35,035 gene-specific 70mere oligonucleotides (Human OligoSet 4.0; Operon, Cologne, Germany) to a set of 35 primary OSCCs. Altogether, 7390 genes were found differentially expressed between OSCC tumor samples and oral mucosa. To characterize the major biologic processes in this tumor collection, MAPPFinder, a component of GenMAPP version 2.1, was applied to this data set to generate a statistically ranked list of molecular signaling pathways. Among others, cancer-related pathways, such as mitogen-activated protein (MAP) kinase signaling (z score = 4.6, $P < .001$), transforming growth factor-beta signaling (z score = 3.0, $P = .015$), and signaling pathways involved in apoptosis (z score = 2.1, $P = .037$), were found deregulated in the OSCC collection analyzed. Focusing on the MAP kinase signaling pathway, subsequent tissue microarray analyses by immunohistochemistry revealed an increase in protein expression of MAP kinase–related proteins ERK1 in 22.8% (48 of 209) and ERK5 in 27.4% (76 of 277), respectively. An association of high ERK5 but not of high ERK1 expression with advanced tumor stage and the presence of lymph node metastases was found ($P = .008$ and $P = .016$, respectively). Our analysis demonstrates the reliability of the combined approach of gene expression profiling, signaling pathway analyses, and tissue microarray analysis to detect novel distinct molecular aberrations in OSCC.

Neoplasia (2008) 10, 462–470

Introduction

Oral squamous cell carcinoma (OSCC) belongs to the 10 most common human malignancies worldwide, affecting more than 500,000 individuals per year. The 5-year survival rate for OSCC does not exceed 55% [1,2], which is mainly caused by locally aggressive tumor phenotypes [3]. Furthermore, clinicopathological parameters such as the TNM system, which are generally used as basis for therapeutic decisions, frequently fail to predict the biologic behavior of the tumors or the patients' outcome. To improve clinical management of individual patients, there is a strong requirement for a better understanding of molecular events involved in OSCC pathophysiology. Attempts to find biomarkers that identify cancerous lesions had identified several candidate genes associated with OSCC tumor progression, including *p53*, *p16*, *MYC*, *CCND1*, *EGFR*, and *CCNL1* [4–7]. Up to now, however, no single gene was shown to have sufficient diagnostic use to predict the biologic behavior of the tumors. Although those studies

Address all correspondence to: Kolja Freier , Klinik für Mund-Kiefer-Gesichtschirurgie, Universitätsklinikum Heidelberg, Im Neuenheimer Feld 400, D-69120 Heidelberg, Germany. E-mail: Kolja.Freier@med.uni-heidelberg.de

[1]Supported in part by the National Genome Research Network (NGFN2-01GS0460/01GR0418), the Tumorzentrum Heidelberg/Mannheim (FSP1–4), and the Medical Faculty of the University Heidelberg.

[2]This article refers to supplementary materials, which are designated by Tables W1 and W2 and Figure W1 and are available online at www.neoplasia.com.

[3]Both authors contributed equally to this work.

Received 14 January 2008; Revised 18 February 2008; Accepted 18 February 2008

DOI 10.1593/neo.08164

contributed greatly to our current understanding, they did not explain the complexity of this malignancy.

High-throughput gene expression profiling techniques offer a unique mechanism for interrogating transcriptome-wide levels of thousands of genes expression and have proven value in defining gene expression signatures dividable in important subsets of patients, who would otherwise be undetected by conventional prognostication schemes [8,9]. Over the last few years, gene expression profiling using microarray hybridization has provided new insights in carcinogenesis and tumor cell dissemination. More than just focusing on the expression of a few genes, genomic-scale expression profiles allow the investigator to look at genetic expression variability in the context of broader genetic themes and pathways. Likewise, the expression profiles of cancers may provide the identification of specific biochemical pathways that might be targeted by new therapeutic agents.

In this study, we applied gene expression microarray technology to a collection of 35 OSCC specimens and compared the gene expression with a pool of normal oral mucosal biopsies from healthy patients. To identify pathways, which are recurrently affected by differential mRNA expression, the software package MAPPFinder was used [10–12], which allows the integration and procession of microarray data sets into the biologic context of molecular functions. To validate individual candidate genes, which were found upregulated in gene expression profiling analyses, a tissue microarray (TMA) analysis was subsequently performed in a representative collection of 306 clinically well-defined primary OSCC specimens.

Materials and Methods

RNA Expression Profiling

OSCC specimen and control samples. Thirty-five frozen tissue tumor samples were collected from patients with histologic confirmed OSCC after approval by the institutional review board of the Universitätsklinikum Heidelberg and after obtaining informed consent. Tumor samples were cut and stained by hematoxylin-eosin. Only samples containing at least 80% tumor cells were used for further analyses. Six oral mucosa samples collected from healthy donors served as control tissue. Nucleic acid extraction of high–molecular weight RNA from frozen tumor tissue was carried out by ultracentrifugation as described elsewhere in detail [13].

Transcriptome amplification and labeling. Two micrograms of total RNA from each patient and Human Universal Reference RNA (Stratagene, La Jolla, CA) were used in a T7-polymerase–based transcriptome amplification method, which was described elsewhere in detail [14].

70mere oligonucleotide microarrays. A set of 35,035 gene-specific 70mere oligonucleotide probes (Human OligoSet 4.0; Operon, Cologne, Germany) was printed on glass slides coated with epoxy–silane (Schott Nexterion, Jena, Germany). The microarray chip represents approximately 25,100 unique genes and 39,600 transcripts excluding control oligos. A variety of data sources was used to cover the genes from human mitochondrial genome, RNA genes, microRNA genes, the endogenous human viral genes, and the exogenous reporter genes (Operon). Microarray production, prehybridization treatment, hybridization, and posthybridization washes, and data acquisition were performed as described previously [15]. After hybridization and stringent washing, fluorescence intensity images were acquired using a dual-laser scanner (G2505 B; Agilent Technologies, Santa Clara, CA) and were analyzed with the GenePix Pro 6.0 imaging software (Molecular Devices, Union City, CA). All hybridization experiments were repeated with inversely labeled sample and reference.

Data preprocessing. Result files containing all relevant raw data were processed using the in-house–developed ChipYard microarray analysis software (http://www.dkfz.de/genetics/ChipYard/), the statistical programming language R, and packages of the Bioconductor project. Raw fluorescence intensity values were normalized applying variance stabilization. We assessed the quality of all hybridizations by generating scatter plots and gradient plots using the Bioconductor package "limma" (www.bioconductor.org). The raw and normalized data are deposited in the Gene Expression Omnibus database (http://www.ncbi.nlm.nih.gov/geo/; Accession No. GSE10121).

Statistical analysis. After normalization, all gene expression data were analyzed for differences between normal and tumor samples using analysis of variance with Bonferroni multiple testing correction. All genes with a log-value between −1 and 1 were excluded from further analyses. To identify pathways, which were likely to be affected by differentially expression, MAPPFinder, a component of GenMAPP software package version 2.1, was used [10–12]. MAPPFinder produces a statistically ranked list of Gene Ontology (GO) biologic categories associated with each cluster, from which the most significant nonsynonymous groups are listed. MAPPFinder analysis was performed on a set of 96 MAPPs, a representation of a biologic relationship between genes or gene products, calculating the percentage of genes meeting the criterion for each MAPP. A positive z score indicates that there are more genes meeting the criterion in a MAPP than would be expected by random chance. A negative z score indicates that there are fewer genes meeting the criterion than would be expected by random chance.

Quantitative real-time reverse transcriptase–polymerase chain reaction. To validate expression profiling data, mRNA levels of selected candidate genes *TRIO*, *TNFRSF18*, *EGFR*, *MAPK3*, and *MAPK7* were tested by quantitative real-time reverse transcriptase–polymerase chain reaction (RT-PCR). For normalization purposes, mean cDNA expression levels of the housekeeping genes *PGK1* and *LamininB1* were measured. Details of the experimental setup are described elsewhere [16,17]. Primer sequences used in these experiments are listed in Table W1.

Tissue Microarray Analysis

Tumor material and patients' characteristics. Paraffin-embedded tumor specimen of primary OSCC were obtained from the archives of the Institute of Pathology of the University Hospital Heidelberg after approval by the local institutional review board. For all tumor samples, clinical and follow-up data of the patients were available from the Department of Oral and Craniomaxillofacial Surgery of the University Hospital Heidelberg. Mean age of the patients was 61 years at the time of diagnosis. Tumors were staged according to

the TNM system of the International Union against Cancer (UICC). Of 306 tumor specimens available for TMA experiments, 143 tumors were T1/2 and 163 were T3/4 tumors. One hundred twenty-five tumors were graded according to UICC stage I to III and 207 were graded according to stage IV, respectively. One hundred twenty-three tumors presented no regional lymph node metastases at the time of diagnosis, whereas 183 exhibited regional lymph node metastases.

Tissue microarray generation. The OSCC-TMA was generated as previously described [18]. Briefly, hematoxylin-eosin–stained sections were cut from each donor block to define representative tumor regions. Small tissue cylinders with a diameter of 0.6 mm were taken from selected areas of each donor block using a tissue chip microarrayer (Beecher Instruments, Silver Spring, MD) and were transferred to a recipient paraffin block. The recipient paraffin block was cut in 5-μm paraffin sections using standard techniques. Five oral mucosa biopsies from healthy donors were incorporated in the recipient block as control specimen.

Immunohistochemistry. The immunohistochemistry (IHC) was performed using the DAKO Real Kit (DAKO; Hamburg, Germany) according to the manufacturer's protocol. Monoclonal mouse antibodies against the phosphorylated forms of ERK1 and ERK5 (Cell Signaling Technology, Beverly, MA) were used at a dilution of 1:1000 for IHC experiments. The primary antibody for phosphorylated ERK1 was the rabbit monoclonal phosphor–p44/42 mitogen-activated protein (MAP) kinase (Thr202/Tyr204) antibody that detects endogenous levels of human p42 and p44 MAP kinase (ERK1 and ERK2) only when they are phosphorylated at Thr202 and Tyr204, respectively. The primary antibody for phosphorylated ERK5 was rabbit phospho-Erk5 (Thr218/Tyr220) antibody that detects endogenous levels of human ERK5 MAP kinase only when they are phosphorylated at Thr218 and Tyr220, respectively. Evaluation of IHC experiments was based on the percentage of cells, which showed distinct nuclear and cytoplasmic staining. Oral mucosa control specimen showed slight nuclear and cytoplasmic staining, which was set as baseline immunoreactivity (0/None) in the following arbitrary score: none, <5% cytoplasmic and nuclear staining; weak, 5% to 30% cytoplasmic and nuclear staining; moderate, 31% to 60% cytoplasmic and nuclear staining; and strong, >60% cytoplasmic and nuclear staining. For statistical analyses, none and weak stainings were combined and counted as low expression, whereas moderate and strong stainings were grouped together and scored as high expression.

Statistical analysis. Nonparametric univariate analysis using chi-square test was performed to compare the prevalence of high ERK1 and ERK5 expression with T-stadium, UICC stage, and the presence of lymph node metastases of the primary tumors. For overall survival, Kaplan–Meier curves of tumors with high *versus* low ERK1 and ERK5 expression were analyzed by log-rank test. $P \leq .05$ was considered significant. All statistical analyses were performed using R for windows version 2.4.1.

Results

70mere Microarray Expression Profiling

In the present study, $n = 35$ tumor specimens of primary OSCCs were analyzed for global gene expression using 70mere oligonucleotide microarrays containing 35,035 gene-specific 70mere oligonucleotides. After quality control, an analysis of variance and a following Bonferroni multitest were performed for the identification of differential gene expression between normal tissue and tumor samples. Gene expression was considered as significantly changed, if exceeding the multiple testing cutoff, computed in this case with $-\log10(P)$ of 5.65 according to the Bonferroni criterion. Using this approach, we identified 7390 genes significantly and differentially expressed between OSCC and normal oral mucosa (Table W2).

Pathway Analysis

To obtain a comprehensive view of global gene expression in OSCC, pathway analysis was applied to this data set of 7390 genes to identify molecular pathways that contained a number of altered transcript levels in OSCC compared to healthy mucosa. MAPPFinder, a component of the software package GenMAPP version 2.1 containing 96 MAPPs, was used. We ran the MAPPFinder analysis on this data set using two criteria, either an increase (fold change > 1 and $-\log10(P) > 5.65$) or a decrease (fold change < −1 and $-\log10(P) > 5.65$) in gene expression to obtain pathways with mostly upregulated genes and pathways with mostly downregulated genes. A pathway was defined as significantly affected by differentially expressed genes, if $P \leq .05$.

In this respect, several significantly altered pathways were revealed with this approach. We found an amount of twenty-three deregulated pathways with MAPPFinder (Table 1). Of those pathways, which were upregulated in the tumor samples analyzed, several were related to inflammatory response system [B cell receptor, $P < .001$; interleukin (IL) 5, $P < .001$; IL-7, $P < .001$; IL-2, $P < .001$; tumor necrosis factor alpha (TNFα)–nuclear factor kappa B (NF-κB), $P < .001$; IL-6, $P = .004$; IL-4, $P = .019$; T cell receptor, $P = .035$]. Other pathways with a high number of differentially expressed genes were cancer-related like MAP kinase signaling ($P < .001$; Figure 1), transforming growth factor-beta (TGF-β) signaling ($P = .015$), and signaling pathways involved in apoptosis ($P = .037$). Pathways with significantly downregulated genes were the ribosomal protein pathway ($P < .001$) and the pathway of members of the electron transport chain ($P < .001$). The MAP kinase signaling pathway exhibited the highest number of altered genes. The altered expressed genes of this pathway are listed in Table 2.

Quantitative Real-Time RT-PCR

To confirm the findings of the microarray analysis, we performed quantitative real-time RT-PCR using primers specific for *TRIO*, *TNFRSF18*, *EGFR*, *MAPK3/ERK1*, and *MAPK7/ERK5*. The fold differences in expression between tumor specimen and control mucosa specimen predicted by 70mere microarray expression profiling were compared to those fold differences obtained by RT-PCR (see Figure W1).

Quantitative PCR confirmed the direction of fold change in 62 (84.9%) of 73 analyses. Overall, these results confirm our findings of differential gene expression by microarray analysis.

Tissue Microarray Analyses

From those pathways found deregulated by cDNA microarray expression profiling in the OSCC tumor samples, further analyses were

Table 1. Identification of Molecular Pathways with Significantly Upregulated (Above) and Downregulated Genes (Below) in OSCC Compared to Healthy Mucosa By MAPPFinder Analysis.

MAPP Name	*n* (Changed)	*n* (Measured)	*n* (on MAPP)	% (Changed)	% (Present)	*z*	*P*
MAPK signaling pathway_	72	151	162	47.7	93.2	4.675	0
TNFα–NF-κB	80	181	187	44.2	96.8	4.096	0
IL-2 NetPath 14	38	75	76	50.7	98.7	3.817	0
IL-7 NetPath 19	25	44	44	56.8	100.0	3.799	0
IL-5 NetPath 17	34	66	69	51.5	95.7	3.726	0
B cell receptor NetPath 12	68	155	158	43.9	98.1	3.681	0
GPCRDB_Other	11	83	119	13.3	69.7	−3.484	0
GPCRDB class rhodopsin-like	27	212	262	12.7	80.9	−5.873	0
Insulin signaling	65	155	159	41.9	97.5	3.144	.002
IL-6 NetPath 18	42	96	100	43.8	96.0	2.839	.004
p38 MAPK signaling pathway	17	32	34	53.1	94.1	2.777	.006
IL-3 NetPath 15	43	99	101	43.4	98.0	2.816	.007
TGF-β receptor	57	145	151	39.3	96.0	2.331	.015
Proteasome degradation	23	50	61	46.0	82.0	2.38	.017
IL-4 NetPath 16	27	62	62	43.5	100.0	2.233	.019
Peptide GPCRs	10	60	73	16.7	82.2	−2.37	.026
IL-9 NetPath 20	12	23	24	52.2	95.8	2.252	.032
T cell receptor NetPath 11	50	129	135	38.8	95.6	2.053	.035
mRNA processing reactome	48	121	127	39.7	95.3	2.207	.036
Apoptosis	33	80	82	41.3	97.6	2.092	.037
Fas pathway and stress induction	17	36	38	47.2	94.7	2.175	.041
Fatty acid beta oxidation 3	5	8	8	62.5	100.0	1.959	.046
Ribosomal_Proteins	35	84	88	41.7	95.5	15.668	0
Electron transport chain	21	103	105	20.4	98.1	7.309	0

focused on the MAP kinase signaling pathway, because MAP kinase signaling is supposed to be critically involved in a variety of cancer-specific functions, such as proliferation, dedifferentiation, and evasion from apoptosis. For TMA analysis, antibodies against ERK1 and ERK5, which play a central role in signal transduction in the MAP kinase signaling pathway, were selected. To test whether OSCC also show an increase of ERK1 and ERK5 protein expression, an immunohistochemical analysis was performed on TMA sections (Figure 2). To assess the functional properties of these proteins in the primary tumor tissue, antibodies against the active phosphorylated form of ERK1 and ERK5 were used. The overall frequency of high pERK5 expression was 27.4% (79 of 277). There was a significantly higher prevalence for high pERK5 expression in T1/2 *versus* T3/4 tumors (P = .015), in Stage I to III *versus* Stage IV tumors (P = .008),

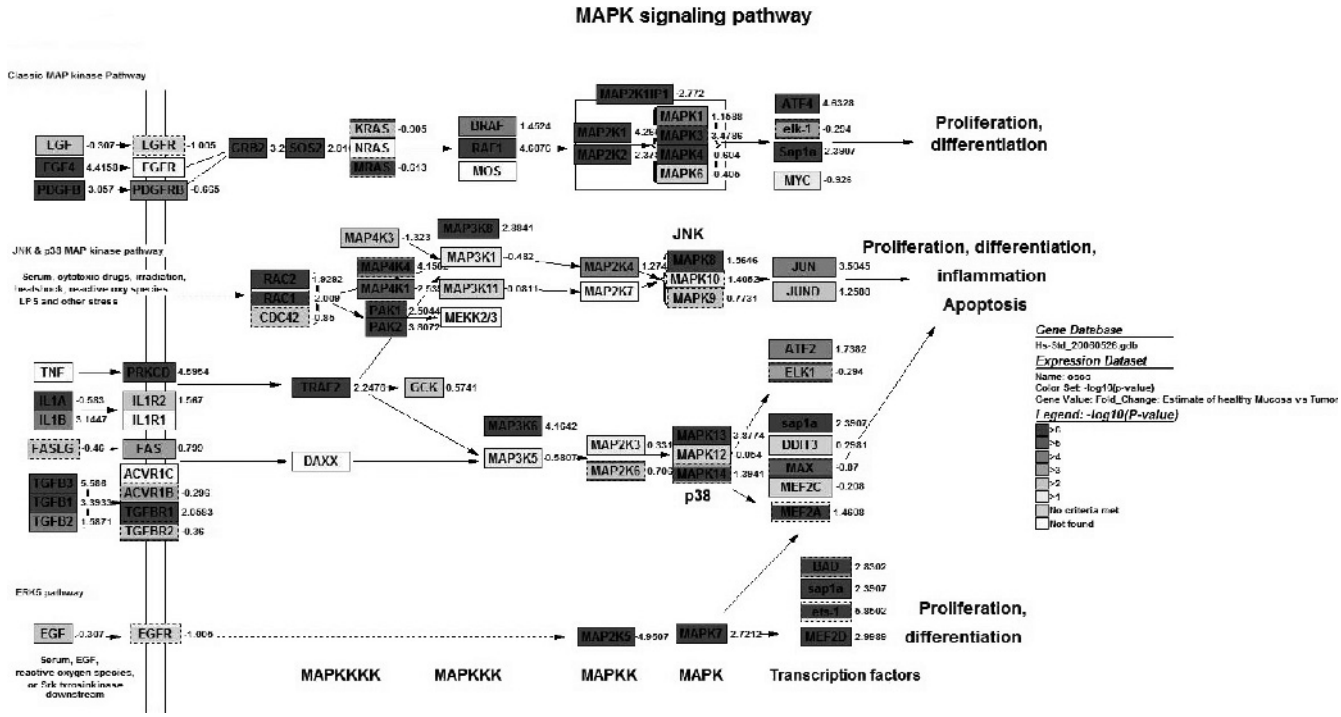

Figure 1. Overview of differentially expressed genes in 35 OSCC compared to six healthy mucosa specimen involved in MAP kinase signaling (modified from the KEGG MAPK pathway). Dark gray color of gene symbols represents the significance of difference [−log10 (*P*)]; the corresponding numbers are the average fold change (log fold).

and for tumors with lymph node metastasis (N1–3) *versus* tumors without lymph node metastasis (N0, $P = .016$). For high pERK1 expression, the overall frequency was 22.8% (48 of 209) without obtaining any correlation of high pERK1 expression with the clinical parameters analyzed. All data obtained from TMA analyses are shown in Table 3. Kaplan–Meier analysis revealed no difference in the overall survival for tumors with high expression *versus* low/no expression of the proteins analyzed ($P > .05$, data not shown).

Discussion

Gene expression profiling to OSCC specimen using different types of cDNA arrays has been performed in several studies to define distinct expression signatures for specific clinical stages [19,20]. To actually understand the process of OSCC progression and metastases, however, it would be essential to know which biologic aberrations are represented by these classifying genes and to what extent they contribute to tumorigenesis. To obtain a comprehensive overview of activated signal transduction pathways in biologic systems, several programs have been developed, which allow the integration and procession of microarray data sets into the context of molecular functions and interrelated dependencies of annotated genes [21–23]. In contrast to those approaches, however, which mainly focus on well-defined metabolic pathways, the program MAPPFinder, which was used in the present analysis, is closely linked to a broader base of pathway information provided by the GO Consortium [11,12]. MAPPFinder dynamically links gene expression data to the GO hierarchy at the level of biologic processes, thereby making it a valuable tool to define novel aberrant pathways in homogenous cohorts of tumor samples [24].

In the present study, a whole-transcriptome expression analysis was performed for 35 OSCC specimens resulting in 7390 differentially expressed transcripts compared to a pool of healthy mucosa samples. By subsequent pathway analysis using MAPPFinder, 24 aberrantly expressed molecular pathways were detected. Among the cancer-related pathways in this data set, most distinct aberrations—mostly upregulations—were found in the MAP kinase signaling network. The MAP kinase signaling pathways are involved in various cellular functions, including cell proliferation, differentiation, and migration by the activation of protooncogenes such as *JUN*, *FOS*, *MYC*, and *ELK1* (Figure 1). Four MAP kinase signaling pathways have been identified, namely, the ERK1 pathway, the c-*jun* N-terminal–regulated kinase (JNK) pathway, the p38 pathway, and the ERK5 pathway [25]. Whereas the JNK and the p38 pathway are signaling cascades, which are mainly stress-activated by proinflammatory cytokines, ERK1 and ERK5 are additionally induced by epidermal growth factor receptor (EGFR) activation [26]. Because EGFR activation is known to be decisively involved in head and neck squamous cell carcinoma (HNSCC) initiation and progression [27], subsequent analyses were focused on ERK1 and ERK5 signaling pathways in the present study. High ERK1 expression and an association with tumor progression and adverse clinical outcome had been observed in several tumor entities, e.g. in primary hepatocellular carcinoma [28], cholangiocarcinoma [29], breast cancer [30], and non–small cell lung cancer [31]. For HNSCC, an involvement of ERK1 signaling in angiogenic processes through vascular endothelial growth factor activation was postulated [32]. In our present TMA analysis, high ERK1 protein expression was found in about 20% of primary OSCC tumor samples. Surprisingly, however, an association with clinical parameters such as advanced UICC stage and presence of lymph node metastases was not found for high ERK1 but for high ERK5 protein expression, although ERK1 and ERK5 coexpression was frequently found. Mitogen signal–regulated ERK5 overexpression was shown to be associated with metastatic prostate cancer [33], but for HNSCC or OSCC, a participation of ERK5 expression in tumor progression has not yet been described. Analyses of tumor cell systems, however, suggested that MAP kinase signaling through ERK5 is a distinct molecular pathway, which might regulate cellular functions such as the activation of protooncogenes originally attributed to ERK1 [34]. Furthermore, it could be shown that ERK5 but not ERK1 signaling contributes to Src-mediated disruption of actin cytoskeleton organization [35]. Because the disorganization of the cytoskeleton is known to be one of the initial steps that are required for the development of metastases, this observation is in concordance with our data of a correlation of high ERK5 expression and the presence of lymph node metastases in OSCC. Therefore, one might speculate that ERK5 signaling is more important in the EGFR-mediated metastasizing process in OSCC than in the classic ERK1 signaling pathway.

A further distinct finding in signaling pathway analysis of the expression profiling data obtained from the OSCC collection was frequently upregulated pathways involved in inflammatory response, e.g., B cell receptor signaling, TNFα signaling, IL-2 signaling, IL-5 signaling, and T cell receptor signaling (Table 1). In general, it is a well-investigated phenomenon that inflammation plays an important role in tumor promotion, particularly in HNSCC development [36]. It was recently postulated that tumor cells can modify the surrounding stroma through the production of cytokines and growth factors and that this locally changed host microenvironment influences the proliferative and invasive behavior of tumor cells [37]. Particularly for HNSCC, it has been demonstrated that primary tumors express a variety of proinflammatory cytokines, including IL-1a, IL-6, IL-8, and granulocyte macrophage colony–stimulating factor that may attract immune effector cells to the tumor microenvironment [38]. In this context, one might interpret the results of the pathway analysis, which showed an increased expression of proinflammatory molecules in the tumor biopsies, as a distinct tumor-specific feature involved in the pathogenesis of the infiltrating process. Conversely, however, inflammatory cytokines are also expressed by cells of the immune system themselves during such an inflammatory process. Therefore, the inflammatory cell infiltration at the invasion front of the tumor might be the source of high cytokine expression as well. Although only tumor samples containing at least 80% tumor cell load in the biopsy were used for expression profiling analysis in the present study, a contamination with cells of the immune system cannot be definitely excluded. Nevertheless, with the development of more efficient microdissection techniques and RNA amplification protocols, a whole-transcriptome expression profiling with smaller RNA samples would be possible. Then, a comprehensive signaling pathway analysis of the expression of immunomodulatory molecules might be a promising approach to further define the role of inflammation in OSCC progression.

Furthermore, pathway analyses showed a significant upregulation of apoptosis-related genes. Although evading apoptosis is a hallmark of almost all malignant tumors, little is known about the actual role of apoptosis-related genes in OSCC development. Previous analyses, for example, suggested increased levels of the anti-apoptotic protein bcl-2 in OSCC samples [39–41]. A recent study, however, using an animal model system exhibiting chemically induced OSCC, found a

Table 2. Increased Expression of Genes Involved in MAP-Kinase Signaling Pathway in 35 OSCC Samples Compared to Six Healthy Mucosa Specimens.

Ensembl ID	Gene Symbol	Gene Name	–log10(*P*)	log (Fold Change)
ENSG00000100311	*PDGFB*	Platelet-derived growth factor B chain precursor	15.467	3.05696878
ENSG00000180370	*PAK2*	Serine/threonine–protein kinase PAK 2	14.294	3.807238826
ENSG00000107566	*CHUK*	SPFH domain-containing protein 1 precursor	14.274	4.832758228
ENSG00000114738	*MAPKAPK3*	MAP kinase–activated protein kinase 3	14.104	4.067114259
ENSG00000089022	*MAPKAPK5*	MAP kinase–activated protein kinase 5	12.030	2.129482743
ENSG00000137764	*MAP2K5*	Dual-specificity mitogen–activated protein kinase kinase 5	11.859	4.950684923
ENSG00000105221	*AKT2*	RAC-beta serine/threonine–protein kinase	11.838	5.375739428
ENSG00000154229	*PRKCA*	Protein kinase C alpha type	11.549	2.137398935
ENSG00000119699	*TGFB3*	Transforming growth factor beta-3 precursor	11.317	5.585986774
ENSG00000166484	*MAPK7*	Mitogen-activated protein kinase 7	11.211	2.721242004
ENSG00000105550	*FGF21*	Fibroblast growth factor 21 precursor (FGF-21)	11.099	1.828757871
ENSG00000167193	*CRK*	Protooncogene C-crk	10.696	4.945734007
ENSG00000142208	*AKT1*	RAC-alpha serine/threonine–protein	10.577	4.734240647
ENSG00000108861	*DUSP3*	Dual-specificity protein phosphatase 3	10.476	3.187181556
ENSG00000115953	*PPP3R1*	Calcineurin subunit B isoform 1	10.403	1.687353652
ENSG00000156711	*MAPK13*	Mitogen-activated protein kinase 13	9.925	3.877349348
ENSG00000085276	*EVI1*	Ecotropic virus integration 1 site protein	9.862	1.102867786
ENSG00000099725	*PRKY*	Serine/threonine–protein kinase PRKY	9.857	4.186894009
ENSG00000126458	*RRAS*	Ras-related protein R-Ras	9.828	3.738753854
ENSG00000142733	*MAP3K6*	Mitogen-activated protein kinase kinase kinase 6	9.684	4.164230763
ENSG00000112658	*SRF*	Serum response factor	9.667	2.390663287
ENSG00000169032	*MAP2K1*	Dual-specificity mitogen-activated protein kinase kinase 1	9.664	4.265539167
ENSG00000112062	*MAPK14*	Mitogen-activated protein kinase 14	9.647	1.394125597
ENSG00000138794	*CASP6*	Caspase-6 precursor	9.462	2.734601578
ENSG00000149269	*PAK1*	Serine/threonine–protein kinase PAK 1	9.420	2.504398448
ENSG00000106799	*TGFBR1*	TGF-beta receptor type I precursor	9.414	2.058273508
ENSG00000174775	*HRAS*	GTPase HRas precursor	9.398	5.345430439
ENSG00000104365	*IKBKB*	Inhibitor of nuclear factor kappa B kinase beta subunit	9.303	2.735869467
ENSG00000162889	*MAPKAPK2*	MAP kinase–activated protein kinase 2	9.128	3.689152094
ENSG00000109971	*HSPA8*	Heat shock cognate 71 kDa protein	9.061	4.628190782
ENSG00000077782	*FGFR1*	Basic fibroblast growth factor receptor 1 precursor	9.035	4.913382054
ENSG00000075429	*CACNG5*	Voltage-dependent calcium channel gamma-5 subunit	8.976	–1.9493298
ENSG00000127191	*TRAF2*	TNF receptor–associated factor 2	8.954	2.247565686
ENSG00000113013	*HSPA9B*	Stress-70 protein, mitochondrial precursor	8.893	5.378858628
ENSG00000177885	*GRB2*	Growth factor receptor–bound protein 2	8.777	3.249343399
ENSG00000132155	*RAF1*	RAF protooncogene serine/threonine–protein kinase	8.731	4.607548955
ENSG00000011485	*PPP5C*	Serine/threonine–protein phosphatase 5	8.703	2.290087262
ENSG00000071054	*MAP4K4*	Mitogen-activated protein kinase kinase kinase kinase 4	8.438	4.156174225
ENSG00000161326	*DUSP14*	Dual-specificity protein phosphatase 14	8.327	4.528707616
ENSG00000067191	*CACNB1*	Voltage-dependent L-type calcium channel beta-1 subunit	7.982	1.761273845
ENSG00000107643	*MAPK8*	Mitogen-activated protein kinase 8	7.942	1.56455685
ENSG00000106211	*HSPB1*	Heat shock protein beta-1 (HspB1)	7.838	1.440732073
ENSG00000126934	*MAP2K2*	Dual-specificity mitogen-activated protein kinase kinase 2	7.818	2.378935599
ENSG00000140285	*FGF7*	Fibroblast growth factor 7 precursor (FGF-7)	7.738	–1.472920826
ENSG00000120875	*DUSP4*	Dual-specificity protein phosphatase 4	7.623	2.488597455
ENSG00000105329	*TGFB1*	Transforming growth factor beta-1 precursor	7.621	3.393246251
ENSG00000134259	*NGFB*	Beta-nerve growth factor precursor (Beta-NGF)	7.586	1.28841258
ENSG00000075388	*FGF4*	Fibroblast growth factor 4 precursor (FGF-4)	7.549	4.415819419
ENSG00000128272	*ATF4*	Cyclic AMP–dependent transcription factor ATF-4	7.490	4.632776685
ENSG00000126583	*PRKCG*	Protein kinase C gamma type	7.399	2.201198322
ENSG00000166501	*PRKCB1*	Protein kinase C beta type	7.396	2.359630993
ENSG00000132906	*CASP9*	Caspase-9 precursor	7.367	4.394431415
ENSG00000100485	*SOS2*	Son of sevenless homolog 2	7.271	2.816563747
ENSG00000128340	*RAC2*	Ras-related C3 *Botulinum* toxin substrate 2 precursor	7.256	1.929198943
ENSG00000107968	*MAP3K8*	Mitogen-activated protein kinase kinase kinase 8	7.202	2.884100613
ENSG00000138834	*MAPK8IP3*	C-*jun*–amino-terminal kinase-interacting protein 3	7.163	2.707867082
ENSG00000123739	*PLA2G12A*	Group XIIA secretory phospholipase A2 precursor	7.105	–1.889796803
ENSG00000143851	*PTPN7*	Tyrosine-protein phosphatase nonreceptor type 7	6.948	1.921973144
ENSG00000102882	*MAPK3*	Mitogen-activated protein kinase 3	6.906	3.478604152
ENSG00000176697	*BDNF*	Brain-derived neurotrophic factor precursor (BDNF)	6.825	1.762730087
ENSG00000141480	*ARRB2*	Beta-arrestin-2 (Arrestin, beta 2)	6.756	2.512394619
ENSG00000085511	*MAP3K4*	Mitogen-activated protein kinase kinase kinase 4	6.655	1.171686631
ENSG00000186895	*FGF3*	Fibroblast growth factor 3 precursor (FGF-3)	6.651	1.401698475
ENSG00000115904	*SOS1*	Son of sevenless homolog 1	6.630	2.41943162
ENSG00000141510	*TP53*	Tumor suppressor p53-binding protein 1	6.479	2.802984167
ENSG00000073009	*IKBKG*	NF-κB essential modulator (NEMO)	6.358	2.203573687
ENSG00000170458	*CD14*	Monocyte differentiation antigen CD14 precursor	6.330	3.763791737
ENSG00000155903	*RASA2*	Ras GTPase-activating protein 2	6.092	1.297339857
ENSG00000136238	*RAC1*	Ras-related C3 *Botulinum* toxin substrate 1 precursor	6.078	–2.009429284
ENSG00000120129	*DUSP1*	Dual-specificity protein phosphatase 1	6.043	2.637357306
ENSG00000138032	*PPM1B*	Protein phosphatase 2C isoform beta	6.006	3.908525816
ENSG00000058335	*RASGRF1*	Guanine nucleotide–releasing protein	5.905	2.008095195
ENSG00000134853	*PDGFRA*	Alpha platelet–derived growth factor receptor precursor	5.808	1.093708029

Table 2. (*continued*)

Ensembl ID	Gene Symbol	Gene Name	–log10(*P*)	log (Fold Change)
ENSG00000113578	*FGF1*	Fibroblast growth factor 1 precursor (FGF-1)	5.786	2.292817534
ENSG00000135090	*TAOK3*	Serine/threonine–protein kinase TAO3	5.759	2.493439143
ENSG00000072062	*PRKACA*	cAMP-dependent protein kinase, alpha-catalytic subunit	5.661	1.435441441
ENSG00000104814	*MAP4K1*	Mitogen-activated protein kinase kinase kinase kinase 1	5.626	2.539747316
ENSG00000142875	*PRKACB*	cAMP-dependent protein kinase, beta-catalytic subunit	5.604	2.081661093

For each transcript, the mean value of these six mucosa specimens was subtracted. An increased expression was defined if this value was higher than three standard deviations of these six healthy mucosa specimens.

high expression of the proapoptotic protein bax but decreased levels of bcl-2 in early oral cancer specimens [39]. Another study on advanced primary OSCC showed an association of high expression of the antiapoptotic protein survivin, with favorable outcome of the patients [42]. Tissue microarray technology might be helpful to further delineate the precise role of apoptosis-related genes in OSCC initiation and progression.

Whereas most of the aberrant signaling pathways were identified as upregulated, the expression of ribosomal proteins was found as significantly downregulated in the tumor collection analyzed. Furthermore, MAPPFinder analysis defined the highest *z* value for ribosomal protein signaling of all pathways analyzed, indicating that its downregulation might be a decisive aberration in OSCC specimen compared to oral mucosa specimen. Only a few published studies have evaluated the role of cytoplasmic ribosomal proteins in carcinogenesis. Significant changes in the expression of several ribosomal proteins have been reported to occur in colorectal carcinoma [43]. In ovarian tumor cell lines, ribosomal proteins, such as S8, S24, and L32, are much more abundantly expressed in differentiated tumor cells than in less-differentiated ones [44]. For OSCC, a downregulation of some ribosomal proteins were found in a previous cDNA expression profiling study, with the downregulation of ribosomal protein S13 discriminating between metastatic and nonmetastatic OSCC in small tumor collection [45]. Because of the observation that a large number of genes encoding ribosomal protein are downregulated in OSCC in our study, further detailed investigation to prove the significance of such global downregulation is warranted.

Pathway signaling analyses results not only contribute to a better understanding of molecular and cellular functions and the definition of potential biomarkers but also open the gate to novel molecular

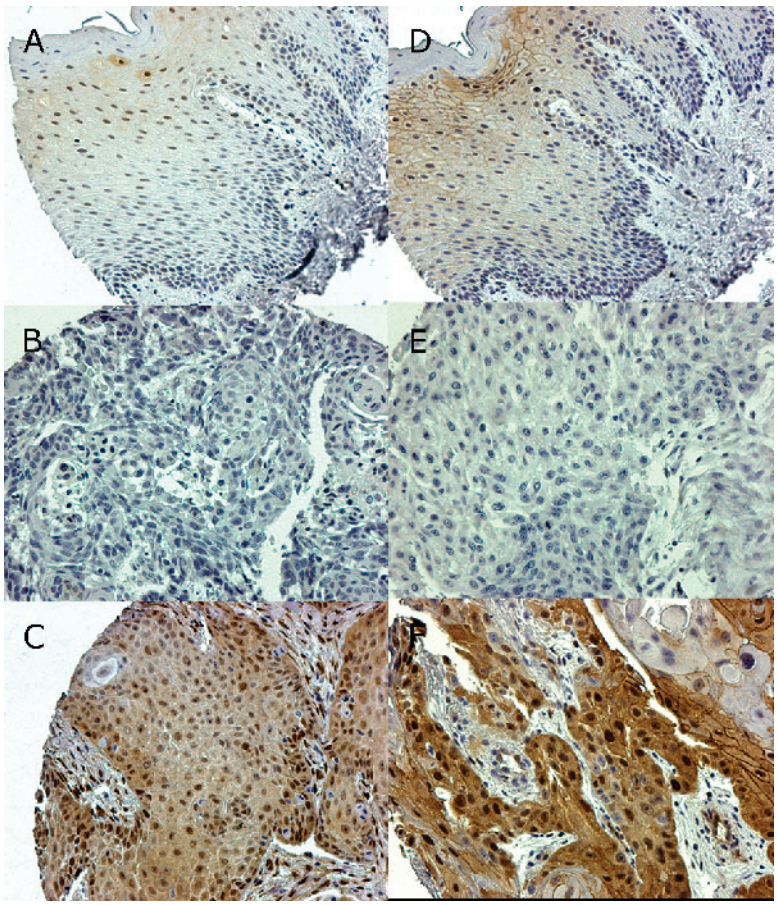

Figure 2. Detection of differential pERK1 (left side) and pERK5 (right side) protein expression on TMA sections as detected by IHC. Normal oral mucosa specimens (A and D; original magnification, ×20) exhibit a slight pERK1 and pERK5 staining. For OSCC specimen, two examples of absent (B and E; original magnification, ×20) and high (C and F; original magnification, ×20) ERK1 and ERK5 protein expression are shown.

Table 3. Frequency of Overexpressed ERK1 and ERK5 in Clinically Defined Tumor Subgroups.

HNSCC (N = 306)	n	ERK1	ERK5
T1/2	143	18.3% (20/109)	20.3% (27/133)
vs			
T3/4	163	28% (28/100)	34% (49/144)
P		.136	.015
N0	124	18.2% (18/99)	19.3% (22/114)
vs			
N1–3	182	27.3% (30/110)	33.1% (54/163)
P		.163	.016
Stages I–III	123	18.0% (16/89)	17.9% (19/106)
vs			
Stage IV	183	26.7% (32/120)	33.3% (57/171)
P		.19	.008

P values for univariate subgroup analysis are added. *P* values ≤ .05 are considered as significant.

targets for specific therapeutic approaches. For ERK1, the negative effect on cell proliferation using specific ERK1 inhibitors has been shown in several tumor systems. In metastasizing neuroblastoma, ERK1 inhibition by the bisphosphonate zoledronic results in a decrease in tumor cell proliferation and an increase in tumor cell apoptosis [46]. For papillary thyroid carcinoma carrying an ERK1-activating *BRAF* mutation, specific ERK1 inhibition resulted in tumor cell growth arrest [47]. Similar effects of tumor cell growth inhibition after blocking ERK1-mediated signaling were found in cholangiocarcinoma [48] and hepatocellular carcinoma [49]. For HNSCC, targeted therapy has been recently established in clinical management by the use of the monoclonal antibody cetuximab that selectively inhibits EGFR. Although cetuximab has proven antitumor activity as a single agent and in combination with radio- and chemotherapy [50], a significant number of patients do not adequately respond to cetuximab treatment. Therefore, it has been postulated that a combination therapy with the additional specific inhibition of downstream mediators of EGFR signaling might be a useful approach to increase cetuximab response [27,51]. In this context, according to the data from the present study, ERK5, as a downstream mediator of EGFR, which is associated with advanced tumor stage, might be a novel molecular target. The use of specific ERK5 inhibitors to block EGFR-induced tumor cell proliferation might be a promising approach to support antitumor activity of cetuximab in HNSCC treatment.

In conclusion, the combined experimental approach of whole-transcriptome expression profiling, automated signaling pathway analysis and protein expression analyses by tissue microarrays resulted in the rapid definition of molecular components, which are critically involved in tumor progression. It allowed the evaluation of diagnostic and prognostic biomarkers as well as the definition of novel promising therapeutic targets. ERK5-mediated signaling of EGFR activation might be more important for OSCC progression than ERK1-mediated signaling, suggesting ERK5 as a potential interference point in future therapeutic approaches.

Acknowledgments

The authors thank Cordula Tschuch, Sebastian Barbus, Daniel Haag, and Frauke Devens for chip printing and technical assistance.

References

[1] Funk GF, Karnell LH, Robinson RA, Zhen WK, Trask DK, and Hoffman HT (2002). Presentation, treatment, and outcome of oral cavity cancer: a National Cancer Data Base report. *Head Neck* **24**, 165–180.

[2] Weinberg MA and Estefan DJ (2002). Assessing oral malignancies. *Am Fam Physician* **65**, 1379–1384.

[3] Jemal A, Murray T, Samuels A, Ghafoor A, Ward E, and Thun MJ (2003). Cancer statistics, 2003. *CA Cancer J Clin* **53**, 5–26.

[4] Sticht C, Hofele C, Flechtenmacher C, Bosch FX, Freier K, Lichter P, and Joos S (2005). Amplification of cyclin L1 is associated with lymph node metastases in head and neck squamous cell carcinoma (HNSCC). *Br J Cancer* **92**, 770–774.

[5] Rodrigo JP, Lazo PS, Ramos S, Alvarez I, and Suarez C (1996). *MYC* amplification in squamous cell carcinomas of the head and neck. *Arch Otolaryngol Head Neck Surg* **122**, 504–507.

[6] Miyaguchi M, Olofsson J, and Hellquist HB (1990). Expression of epidermal growth factor receptor in laryngeal dysplasia and carcinoma. *Acta Otolaryngol* **110**, 309–313.

[7] Boyle JO, Hakim J, Koch W, van der Riet P, Hruban RH, Roa RA, Correo R, Eby YJ, Ruppert JM, and Sidransky D (1993). The incidence of *p53* mutations increases with progression of head and neck cancer. *Cancer Res* **53**, 4477–4480.

[8] Nutt CL, Mani DR, Betensky RA, Tamayo P, Cairncross JG, Ladd C, Pohl U, Hartmann C, McLaughlin ME, Batchelor TT, et al. (2003). Gene expression–based classification of malignant gliomas correlates better with survival than histological classification. *Cancer Res* **63**, 1602–1607.

[9] Alizadeh AA, Eisen MB, Davis RE, Ma C, Lossos IS, Rosenwald A, Boldrick JC, Sabet H, Tran T, Yu X, et al. (2000). Distinct types of diffuse large B-cell lymphoma identified by gene expression profiling. *Nature* **403**, 503–511.

[10] Dahlquist KD, Salomonis N, Vranizan K, Lawlor SC, and Conklin BR (2002). GenMAPP, a new tool for viewing and analyzing microarray data on biological pathways. *Nat Genet* **31**, 19–20.

[11] Ashburner M, Ball CA, Blake JA, Botstein D, Butler H, Cherry JM, Davis AP, Dolinski K, Dwight SS, Eppig JT, et al. (2000). Gene ontology: tool for the unification of biology. The Gene Ontology Consortium. *Nat Genet* **25**, 25–29.

[12] Doniger SW, Salomonis N, Dahlquist KD, Vranizan K, Lawlor SC, and Conklin BR (2003). MAPPFinder: using Gene Ontology and GenMAPP to create a global gene-expression profile from microarray data. *Genome Biol* **4**, R7.

[13] van den Boom J, Wolter M, Kuick R, Misek DE, Youkilis AS, Wechsler DS, Sommer C, Reifenberger G, and Hanash SM (2003). Characterization of gene expression profiles associated with glioma progression using oligonucleotide-based microarray analysis and real-time reverse transcription–polymerase chain reaction. *Am J Pathol* **163**, 1033–1043.

[14] Schlingemann J, Thuerigen O, Ittrich C, Toedt G, Kramer H, Hahn M, and Lichter P (2005). Effective transcriptome amplification for expression profiling on sense-oriented oligonucleotide microarrays. *Nucleic Acids Res* **33**, e29.

[15] Tews B, Felsberg J, Hartmann C, Kunitz A, Hahn M, Toedt G, Neben K, Hummerich L, von Deimling A, Reifenberger G, et al. (2006). Identification of novel oligodendroglioma-associated candidate tumor suppressor genes in 1p36 and 19q13 using microarray-based expression profiling. *Int J Cancer* **119**, 792–800.

[16] Korz C, Pscherer A, Benner A, Mertens D, Schaffner C, Leupolt E, Dohner H, Stilgenbauer S, and Lichter P (2002). Evidence for distinct pathomechanisms in B-cell chronic lymphocytic leukemia and mantle cell lymphoma by quantitative expression analysis of cell cycle and apoptosis-associated genes. *Blood* **99**, 4554–4561.

[17] Schwaenen C, Nessling M, Wessendorf S, Salvi T, Wrobel G, Radlwimmer B, Kestler HA, Haslinger C, Stilgenbauer S, Dohner H, et al. (2004). Automated array-based genomic profiling in chronic lymphocytic leukemia: development of a clinical tool and discovery of recurrent genomic alterations. *Proc Natl Acad Sci USA* **101**, 1039–1044.

[18] Freier K, Bosch FX, Flechtenmacher C, Devens F, Benner A, Lichter P, Joos S, and Hofele C (2003). Distinct site-specific oncoprotein overexpression in head and neck squamous cell carcinoma: a tissue microarray analysis. *Anticancer Res* **23**, 3971–3977.

[19] O'Donnell RK, Kupferman M, Wei SJ, Singhal S, Weber R, O'Malley B, Cheng Y, Putt M, Feldman M, Ziober B, et al. (2005). Gene expression signature predicts lymphatic metastasis in squamous cell carcinoma of the oral cavity. *Oncogene* **24**, 1244–1251.

[20] Nagata M, Fujita H, Ida H, Hoshina H, Inoue T, Seki Y, Ohnishi M, Ohyama T, Shingaki S, Kaji M, et al. (2003). Identification of potential biomarkers of lymph node metastasis in oral squamous cell carcinoma by cDNA microarray analysis. *Int J Cancer* **106**, 683–689.

[21] Karp PD, Riley M, Paley SM, and Pellegrini-Toole A (2002). The MetaCyc database. *Nucleic Acids Res* **30**, 59–61.

[22] Grosu P, Townsend JP, Hartl DL, and Cavalieri D (2002). Pathway processor: a tool for integrating whole-genome expression results into metabolic networks. *Genome Res* **12**, 1121–1126.

[23] Luyf AC, de Gast J, and van Kampen AH (2002). Visualizing metabolic activity on a genome-wide scale. *Bioinformatics* **18**, 813–818.

[24] Zucchini C, Bianchini M, Valvassori L, Perdichizzi S, Benini S, Manara MC, Solmi R, Strippoli P, Picci P, Carinci P, et al. (2004). Identification of candidate genes involved in the reversal of malignant phenotype of osteosarcoma cells transfected with the liver/bone/kidney alkaline phosphatase gene. *Bone* **34**, 672–679.

[25] Garrington TP and Johnson GL (1999). Organization and regulation of mitogen-activated protein kinase signaling pathways. *Curr Opin Cell Biol* **11**, 211–218.

[26] Kato Y, Tapping RI, Huang S, Watson MH, Ulevitch RJ, and Lee JD (1998). Bmk1/Erk5 is required for cell proliferation induced by epidermal growth factor. *Nature* **395**, 713–716.

[27] Kalyankrishna S and Grandis JR (2006). Epidermal growth factor receptor biology in head and neck cancer. *J Clin Oncol* **24**, 2666–2672.

[28] Tsuboi Y, Ichida T, Sugitani S, Genda T, Inayoshi J, Takamura M, Matsuda Y, Nomoto M, and Aoyagi Y (2004). Overexpression of extracellular signal–regulated protein kinase and its correlation with proliferation in human hepatocellular carcinoma. *Liver Int* **24**, 432–436.

[29] Jinawath A, Akiyama Y, Yuasa Y, and Pairojkul C (2006). Expression of phosphorylated ERK1/2 and homeodomain protein CDX2 in cholangiocarcinoma. *J Cancer Res Clin Oncol* **132**, 805–810.

[30] Milde-Langosch K, Bamberger AM, Rieck G, Grund D, Hemminger G, Muller V, and Loning T (2005). Expression and prognostic relevance of activated extracellular-regulated kinases (ERK1/2) in breast cancer. *Br J Cancer* **92**, 2206–2215.

[31] Vicent S, Lopez-Picazo JM, Toledo G, Lozano MD, Torre W, Garcia-Corchon C, Quero C, Soria JC, Martin-Algarra S, Manzano RG, et al. (2004). ERK1/2 is activated in non–small-cell lung cancer and associated with advanced tumours. *Br J Cancer* **90**, 1047–1052.

[32] Bancroft CC, Chen Z, Dong G, Sunwoo JB, Yeh N, Park C, and Van Waes C (2001). Coexpression of proangiogenic factors IL-8 and VEGF by human head and neck squamous cell carcinoma involves coactivation by MEK-MAPK and IKK–NF-kappaB signal pathways. *Clin Cancer Res* **7**, 435–442.

[33] Mehta PB, Jenkins BL, McCarthy L, Thilak L, Robson CN, Neal DE, and Leung HY (2003). MEK5 overexpression is associated with metastatic prostate cancer, and stimulates proliferation, MMP-9 expression and invasion. *Oncogene* **22**, 1381–1389.

[34] Wang X and Tournier C (2006). Regulation of cellular functions by the ERK5 signalling pathway. *Cell Signal* **18**, 753–760.

[35] Nishimoto S and Nishida E (2006). MAPK signalling: ERK5 *versus* ERK1/2. *EMBO Rep* **7**, 782–786.

[36] Gleich LL and Salamone FN (2002). Molecular genetics of head and neck cancer. *Cancer Control* **9**, 369–378.

[37] Pupa SM, Menard S, Forti S, and Tagliabue E (2002). New insights into the role of extracellular matrix during tumor onset and progression. *J Cell Physiol* **192**, 259–267.

[38] Chen Z, Malhotra PS, Thomas GR, Ondrey FG, Duffey DC, Smith CW, Enamorado I, Yeh NT, Kroog GS, Rudy S, et al. (1999). Expression of proinflammatory and proangiogenic cytokines in patients with head and neck cancer. *Clin Cancer Res* **5**, 1369–1379.

[39] Derka S, Vairaktaris E, Papakosta V, Vassiliou S, Acil Y, Vylliotis A, Spyridonidou S, Lazaris AC, Mourouzis C, Kokkori A, et al. (2006). Cell proliferation and apoptosis culminate in early stages of oral oncogenesis. *Oral Oncol* **42**, 540–550.

[40] Loro LL, Vintermyr OK, Liavaag PG, Jonsson R, and Johannessen AC (1999). Oral squamous cell carcinoma is associated with decreased bcl-2/bax expression ratio and increased apoptosis. *Hum Pathol* **30**, 1097–1105.

[41] Singh BB, Chandler FW Jr, Whitaker SB, and Forbes-Nelson AE (1998). Immunohistochemical evaluation of bcl-2 oncoprotein in oral dysplasia and carcinoma. *Oral Surg Oral Med Oral Pathol Oral Radiol Endod* **85**, 692–698.

[42] Freier K, Pungs S, Sticht C, Flechtenmacher C, Lichter P, Joos S, and Hofele C (2007). High survivin expression is associated with favorable outcome in advanced primary oral squamous cell carcinoma after radiation therapy. *Int J Cancer* **120**, 942–946.

[43] Kasai H, Nadano D, Hidaka E, Higuchi K, Kawakubo M, Sato TA, and Nakayama J (2003). Differential expression of ribosomal proteins in human normal and neoplastic colorectum. *J Histochem Cytochem* **51**, 567–574.

[44] Welsh JB, Zarrinkar PP, Sapinoso LM, Kern SG, Behling CA, Monk BJ, Lockhart DJ, Burger RA, and Hampton GM (2001). Analysis of gene expression profiles in normal and neoplastic ovarian tissue samples identifies candidate molecular markers of epithelial ovarian cancer. *Proc Natl Acad Sci USA* **98**, 1176–1181.

[45] Mendez E, Cheng C, Farwell DG, Ricks S, Agoff SN, Futran ND, Weymuller EA Jr, Maronian NC, Zhao LP, and Chen C (2002). Transcriptional expression profiles of oral squamous cell carcinomas. *Cancer* **95**, 1482–1494.

[46] Peng H, Sohara Y, Moats RA, Nelson MD Jr, Groshen SG, Ye W, Reynolds CP, and DeClerck YA (2007). The activity of zoledronic acid on neuroblastoma bone metastasis involves inhibition of osteoclasts and tumor cell survival and proliferation. *Cancer Res* **67**, 9346–9355.

[47] Henderson YC, Fredrick MJ, and Clayman GL (2007). Differential responses of human papillary thyroid cancer cell lines carrying the *RET/PTC1* rearrangement or a *BRAF* mutation to MEK1/2 inhibitors. *Arch Otolaryngol Head Neck Surg* **133**, 810–815.

[48] Jinawath A, Akiyama Y, Sripa B, and Yuasa Y (2007). Dual blockade of the Hedgehog and ERK1/2 pathways coordinately decreases proliferation and survival of cholangiocarcinoma cells. *J Cancer Res Clin Oncol* **133**, 271–278.

[49] Schmidt CM, Wang Y, and Wiesenauer C (2003). Novel combination of cyclooxygenase-2 and MEK inhibitors in human hepatocellular carcinoma provides a synergistic increase in apoptosis. *J Gastrointest Surg* **7**, 1024–1033.

[50] Astsaturov I, Cohen RB, and Harari P (2006). Targeting epidermal growth factor receptor signaling in the treatment of head and neck cancer. *Expert Rev Anticancer Ther* **6**, 1179–1193.

[51] Huang S, Armstrong EA, Benavente S, Chinnaiyan P, and Harari PM (2004). Dual-agent molecular targeting of the epidermal growth factor receptor (EGFR): combining anti–EGFR antibody with tyrosine kinase inhibitor. *Cancer Res* **64**, 5355–5362.

Table W1. List of RT-PCR Primer to Validate Expression Profiling Data.

Gene	Forward Primer	Reverse Primer
MAPK3	5′-GCT ACA CGC AGT TGC AGT AC-3′	5′-CAG TAG GTC TGA TGT TCG AAG-3′
MAPK7	5′-ACA TCA TCG CCA TCA AGG ACA T-3′	5′-AGG AAG TAG CGC ACG TGT TC-3′
MAPK8	5′-CTG TGT GGA ATC AAG CAC CTT CA-3′	5′-GTG CTC TGT AGT AGC GAG TCA CT-3′
MAPK9	5′-ATT CAC ATG GAG CTG GAT CAT GA-3′	5′-CCA GGC CAA AGT CAA GGA TCT TC-3′
Trio	5′-CCT CAG AGC TGC AGG ACC TAG-3′	5′-C51CGA CTT CCC ATC TTG GCT GAC-3′
SDF4	5′-CAC GTG TCT TGG GAC GAG TA-3′	5′-CAG GTT CTC CAG GAC TTC CT-3′
FGF3	5′-GTA CCT GGC CAT GAA CAA GAG-3′	5′-CAT ACG TAT TAT AGC CCA GCT CG-3′
EGF	5′-CAC GAT GGG TAC TGC CTC CAT G-3′	5′-GCG CAG TTC CCA CCA CTT-3′
EGFR	5′-CCA CCA CGT ACC AGA TGG ATG T-3′	5′-ACG CAC GAG CCG TGA TC-3′

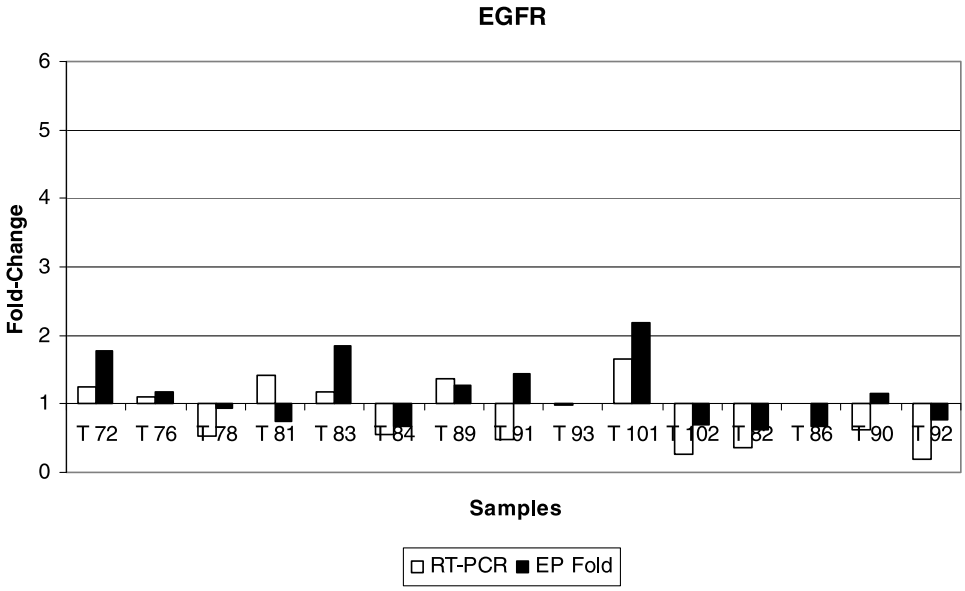

Figure W1. Relative mRNA expression levels (white bars) of *EGFR*, *Trio*, *TNFRSF18*, *MAPK7*, and *MAPK8* in OSCCs with expression profiling results (black bars).

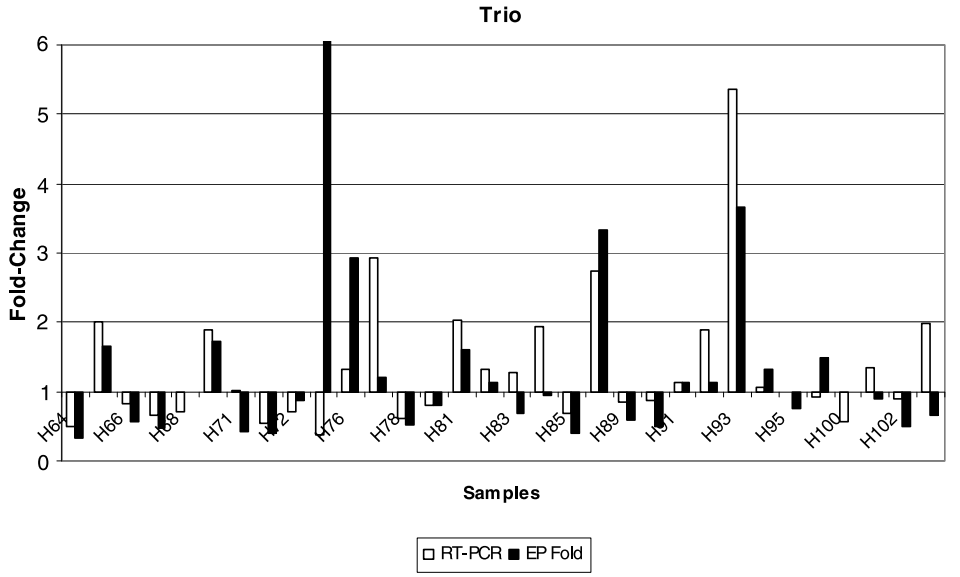

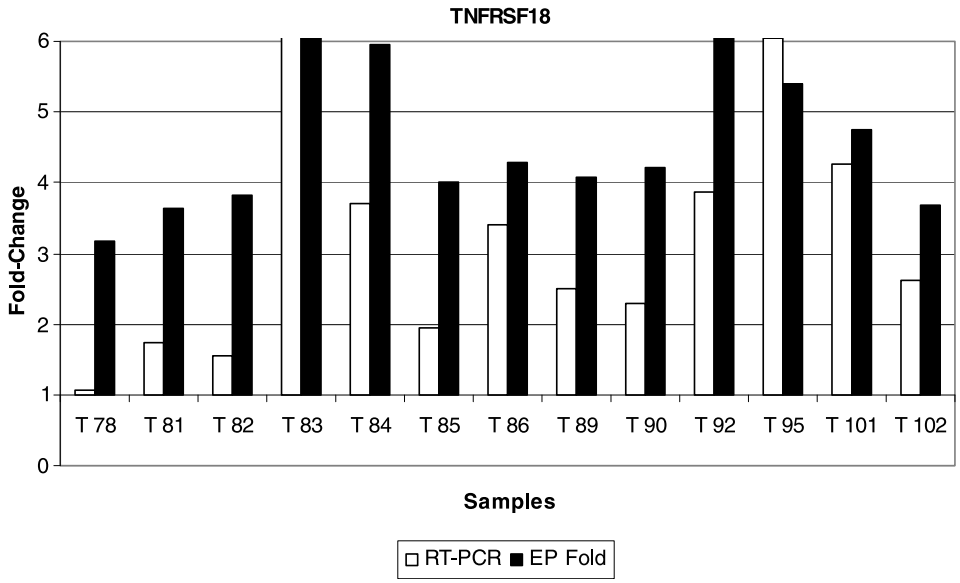

Figure W1. (*continued*).

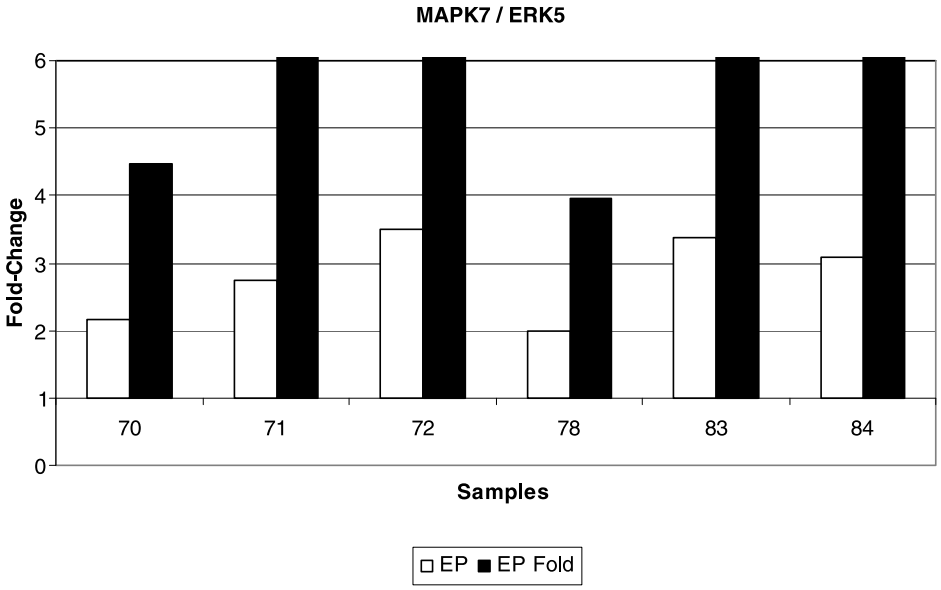

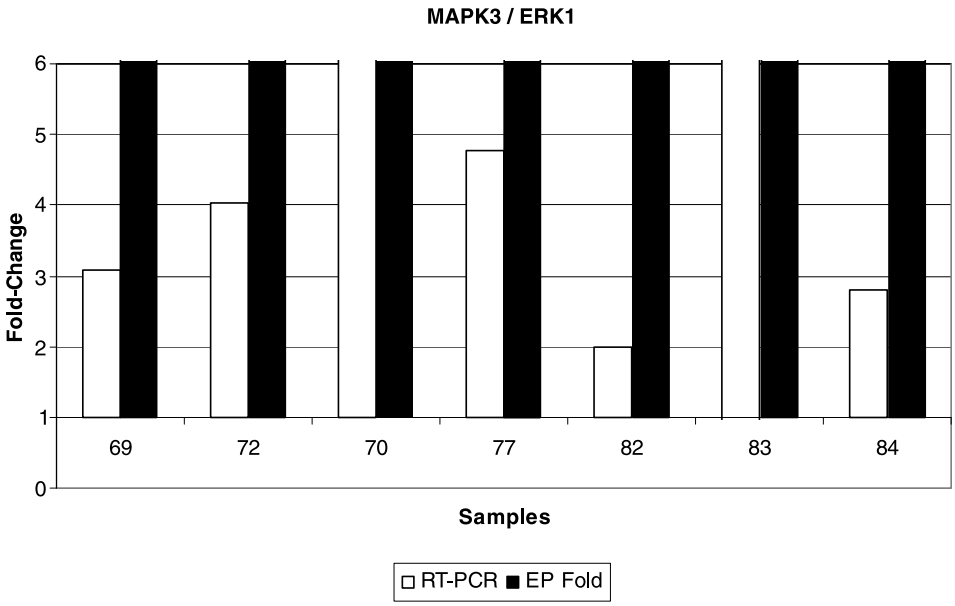

Figure W1. (*continued*).